Differential cross sections for low-energy electron elastic scattering by lanthanide atoms: La, Ce, Pr, Nd, Eu, Gd, Dy, and Tm

Z. Felfli,[1] A. Z. Msezane,[1] and D. Sokolovski[2]
[1]*Department of Physics and Centre for Theoretical Studies of Physical Systems, Clark Atlanta University, Atlanta, Georgia 30314, USA*
[2]*School of Mathematics and Physics, Queen's University of Belfast, Belfast BT7 1NN, United Kingdom*
(Received 4 March 2009; published 12 June 2009)

Elastic differential cross sections (DCSs) in angle of electron scattering by the representative lanthanide atoms La, Ce, Pr, Nd, Eu, Gd, Dy, and Tm have been calculated in the electron-impact energy range $0 \leq E \leq 1$ eV. Additionally, the DCSs in electron-impact energy are also presented at scattering angles $\theta = 0°$, 90°, and 180° for unambiguous identification of the binding energies (BEs) of the negative ions formed during the collisions as resonances. The shape resonances and the DCSs critical minima are identified as well. A Thomas-Fermi-type potential incorporating the vital core-polarization interaction is used for the calculations. Dramatically sharp resonances are found to characterize the near-threshold electron elastic DCSs, whose energy positions are identified with the BEs of the resultant negative ions. A procedure is suggested for measuring reliably the BEs of tenuously bound (BE<0.1 eV), weakly bound (BE<1 eV), and complicated open *d*- and *f*-subshell negative ions through the elastic DCSs both in scattering angle and electron-impact energy.

DOI: 10.1103/PhysRevA.79.062709 PACS number(s): 34.80.Bm

I. INTRODUCTION

In a recent paper [1] the near-threshold electron attachment mechanism in electron-lanthanide atom scattering, manifesting itself as Regge resonances, was investigated using the recently developed Regge-pole analysis through the calculation of the electron elastic total cross sections (TCSs) and the Mulholland partial cross sections [2]. Generally, the TCSs were found to be characterized by dramatically sharp resonance structures whose energy positions were identified with the binding energies (BEs) of the resultant negative ions formed during the collisions as Regge resonances. This is consistent with the conclusion [3] that the existence of a large peak in the electron-atom scattering TCS at low energy represents the signature of the ground state of the negative ion, with the proviso that the second or even the third empty orbital be at low energy and has orbital angular momentum, $l>0$. Indeed, the careful scrutiny of the imaginary part of the complex angular momentum, L, Im L was used [1] to distinguish between the bound states of the negative ions and the shape resonances. For the latter Im L was found to be several orders-of-magnitude greater than that corresponding to the former. Ramsauer-Townsend minima, shape resonances, and the Wigner threshold law were also determined. The BEs extracted from the resonances were compared with those from recent measurements and calculations. In particular, the negative ions whose binding energies agreed very well with the most recently measured and/or calculated values are among those selected for use in the present investigation of the electron elastic differential cross sections (DCSs).

Here we have selected typical lanthanides, determined through their formation of tenuously bound (BE<0.1 eV), weakly bound (BE<1 eV), and complicated open *d*- and *f*-subshell negative ions in the near-threshold electron elastic scattering, to investigate the structure of the DCSs in angle in the electron-impact energy range $0 \leq E \leq 1$ eV. The DCSs in energy at the scattering angles $\theta = 0°$, 90°, and 180° are calculated as well; these readily yield the BEs of the negative ions formed during the collisions [4]. Also determined are the so-called DCS critical minima [5] which correspond to the DCS minima in the plane of scattering angle and projectile energy. The accurate experimental determination of the depth of the critical minimum is virtually impossible due to the finite resolution of an experimental apparatus [6]. The recent experimental investigations of the DCSs and their critical minima in the elastic electron-Kr scattering at intermediate incident electron energies (100–260 eV) and scattering angles (30°–110°) [5], as well as in the elastic electron-Yb scattering at 10, 40, and 80 eV in the angular range $10° \leq \theta \leq 160°$ [7] demonstrate the experimental difficulties and the need for theoretical guidance, particularly as $E \to 0$ eV and $\theta \to 0°$.

It is therefore appropriate to explore the near-threshold electron DCSs for the lanthanides to guide future experimental and theoretical investigations. The DCSs provide stringent test of theoretical calculations when the results are compared with those of reliable measurements. However, for the lanthanides the only available detailed near-threshold electron-scattering data, to our knowledge, are the TCSs and partial cross sections [1]. Also, the published electron DCSs, including the positions of the critical minima, for the lanthanide atoms are only those for Yb by Predojevic *et al.* [7] and Kelemen *et al.* [8] but the former cover the electron energy range $E>10$ eV while for the latter the energy range is 2 eV–2 keV; these are much higher than the energy range of interest here. There are some theoretical and experimental results for *e*-Yb scattering [9] but neither the theory nor the experiment explored the energy region near threshold, i.e., below 0.1 eV. For the energy range $E<2$ eV, comparison between the measured and calculated [9] DCSs for *e*-Yb scattering have been discussed [10]. We note that Remeta *et al.* [11] calculated low-energy, below 2 eV, electron elastic forward and backward scatterings by some atoms, including Ca and Yb, using their optical potential approach. They obtained the total elastic and differential cross sections. However, the adjustable parameter used in the calculation of the

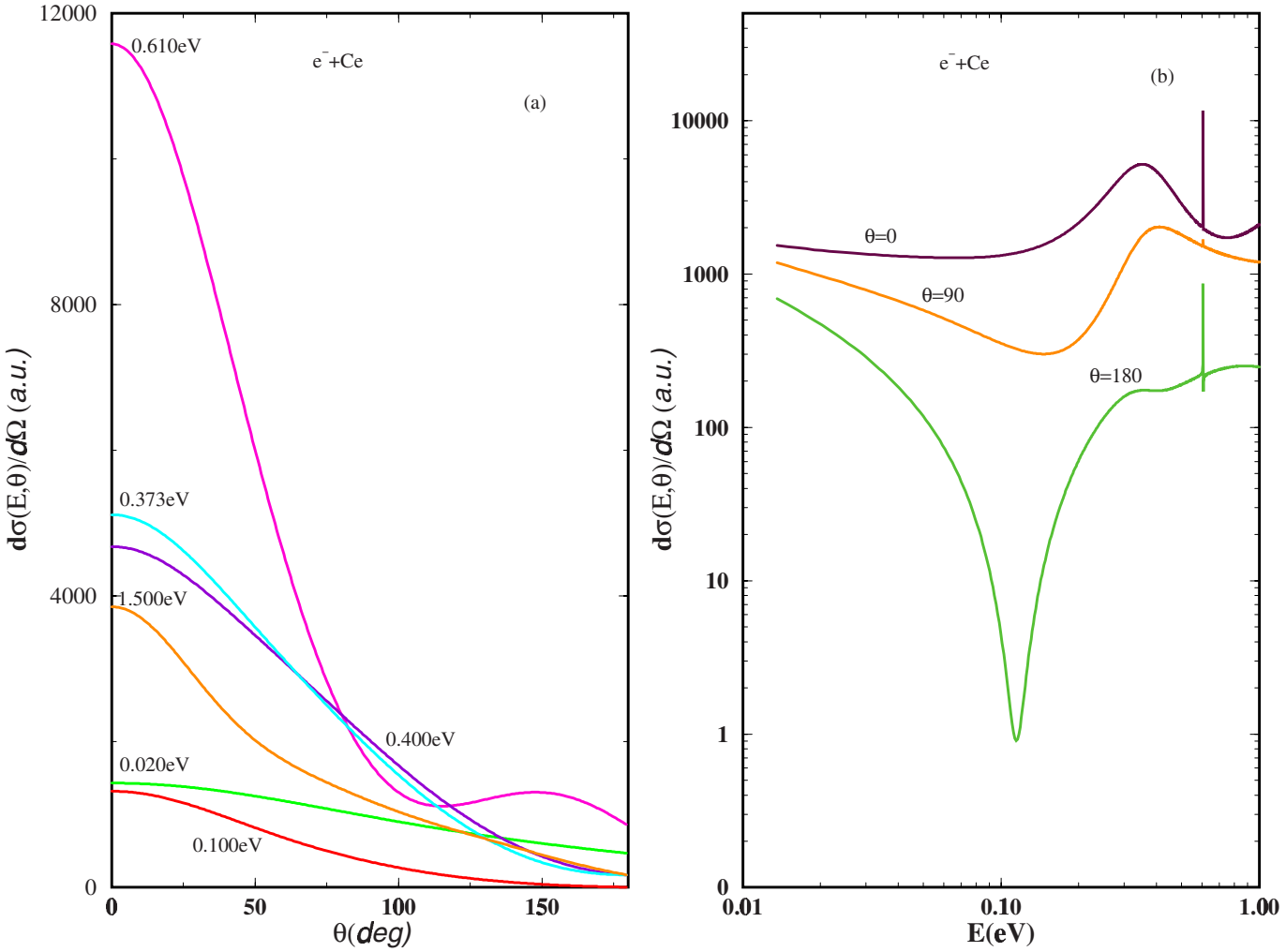

FIG. 1. (Color online) (a) Differential cross sections (a.u.) in scattering angle for electron elastic scattering by Ce atom at impact energies of 0.020, 0.1, 0.373, 0.400, 0.610, and 1.500 eV, showing the strong forward peaking at the binding energy of the resultant negative Ce^- ion. (b) Differential cross sections (a.u.) in impact energy for electron elastic scattering by Ce atom at scattering angles θ=0°, 90°, and 180°. The position of the sharp resonances corresponds to the binding energy of the resultant negative Ce^- ion; the DCS critical minimum is also shown.

phase shifts for Ca and Yb was determined using the old and incorrect values of the electron affinities (EAs), viz. 43 ± 7 and 54 ± 27 meV, respectively; the electron affinity is numerically equal to the binding energy. Consequently, the calculated TCSs and DCSs for these atoms [11] cannot be deemed reliable. Furthermore, the obtained results are not at sufficiently low energies to cover the interesting region of the dramatic resonances, corresponding to the BEs of the negative Ca^- and Yb^- ions [4] formed during the collisions.

The Ce^- and Gd^- negative ions are the most complicated of the lanthanides in the context of both having open f and d subshells. For this reason the EA of Ce has only been determined with confidence recently both theoretically [12,13] and experimentally [14]. However, the EA of the Gd atom, including the TCSs and the partial cross sections, have been calculated only theoretically with confidence very recently [1]. The reason is that generally complex and subtle interactions among the many diverse electron configurations in the lanthanide atoms, particularly in the Ce and Gd atoms, render accurate and reliable structure-based-type calculations very difficult, if not impossible. Generally, the recently calculated values [1] of the EAs of the La, Ce, Nd, Eu, and Tm atoms agree excellently when compared with the latest measured [14,15] and calculated [16,17] results; hence the use of these atoms for the investigations of the near-threshold DCSs.

II. CALCULATIONAL PROCEDURE

For a particle scattered by a central field $U(r)$ the DCS, $d\sigma(E,\theta)/d\Omega$, is given by

$$d\sigma(E,\theta)/d\Omega = |f(E,\theta)|^2, \quad (1)$$

where the scattering amplitude $f(E,\theta)$ can be expressed as a partial-wave sum

$$f(E,\theta) = (1/2ik)\sum_{\ell=0}^{\infty}(2\ell+1)P_\ell(\cos\theta)[S_\ell(E)-1], \quad (2)$$

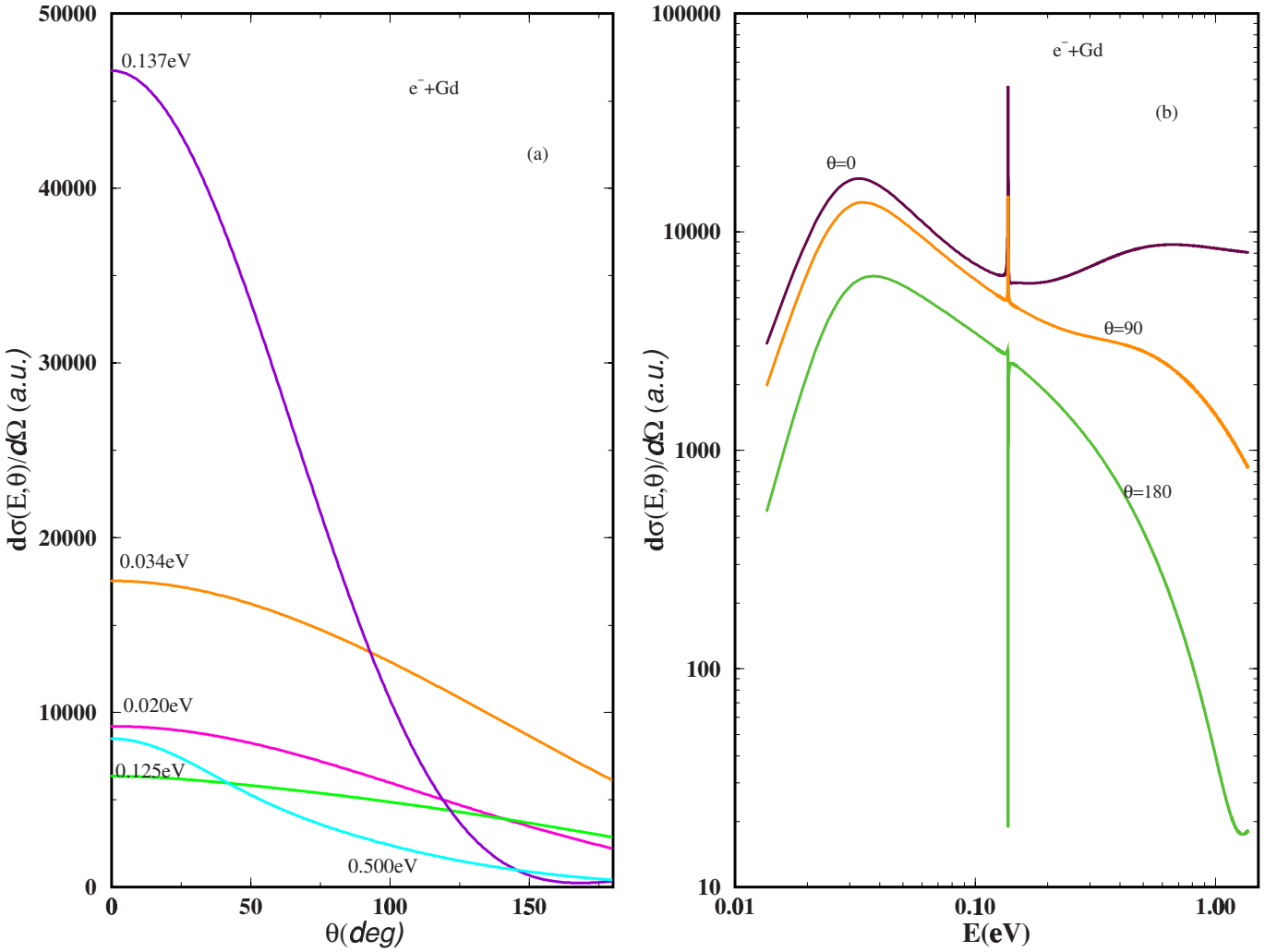

FIG. 2. (Color online) (a) Differential cross sections (a.u.) in scattering angle for electron elastic scattering by Gd atom at impact energies of 0.020, 0.034, 0.125, 0.137, and 0.500 eV, showing the strong forward peaking at the binding energy of the resultant negative Gd^- ion. (b) Differential cross sections (a.u.) in impact energy for electron elastic scattering by Gd atom at scattering angles θ=0°, 90°, and 180°. The position of the sharp resonances corresponds to the binding energy of the resultant negative Gd^- ion; the DCS critical minimum is also shown.

with $k, \ell, \theta, P_\ell(\cos\theta)$, and $S_\ell(E)$ being the wave vector, the angular-momentum quantum number, the scattering angle, a Legendre polynomial of degree ℓ, and the scattering matrix element, respectively. For central field scattering

$$S_\ell(E) = \exp[i\delta(E,\ell)], \tag{3}$$

where $\delta(E,\ell)$ are the phase shifts. We note that in [1] Eq. (2) was recast to yield the Mulholland formula for elastic-scattering total cross section, revealing its pole structure.

For the calculation of the DCSs Eq. (2) was summed over all ℓ. In the present calculation the TF-type potential takes the well investigated [18] in another context and successfully used [1,4,10,13] form

$$U(r) = \frac{-Z}{r(1+aZ^{1/3}r)(1+bZ^{2/3}r^2)}, \tag{4}$$

where Z is the nuclear charge and a and b are adjustable parameters. For small r, the potential describes the Coulomb attraction between an electron and a nucleus, $U(r) \sim -Z/(r)$, while at large distances it mimics the polarization potential, $U(r) \sim -1/(abr^4)$ and accounts properly for the vital core-polarization interaction at very low energies, the energy region of interest of this paper. The effective potential,

$$V(r) = U(r) + \ell(\ell+1)/(2r^2), \tag{5}$$

is considered here as a continuous function of the variables r and ℓ. For ℓ=0, $V(r)$ is a potential well which, due to its short-ranged, $\sim -1/r^4$, asymptotic behavior supports a finite number of bound states, see Ref. [2]. For larger ℓ values, $V(r)$ becomes purely repulsive so that it no longer can support narrow resonances. When the TCS as a function of "b" has a resonance [1] corresponding to the formation of a negative ion, this resonance is longest lived for a given value of the energy which corresponds to the electron affinity of the system. This was found to be the case for all of the systems we have investigated so far [1,4,10,13], including e^--Au,

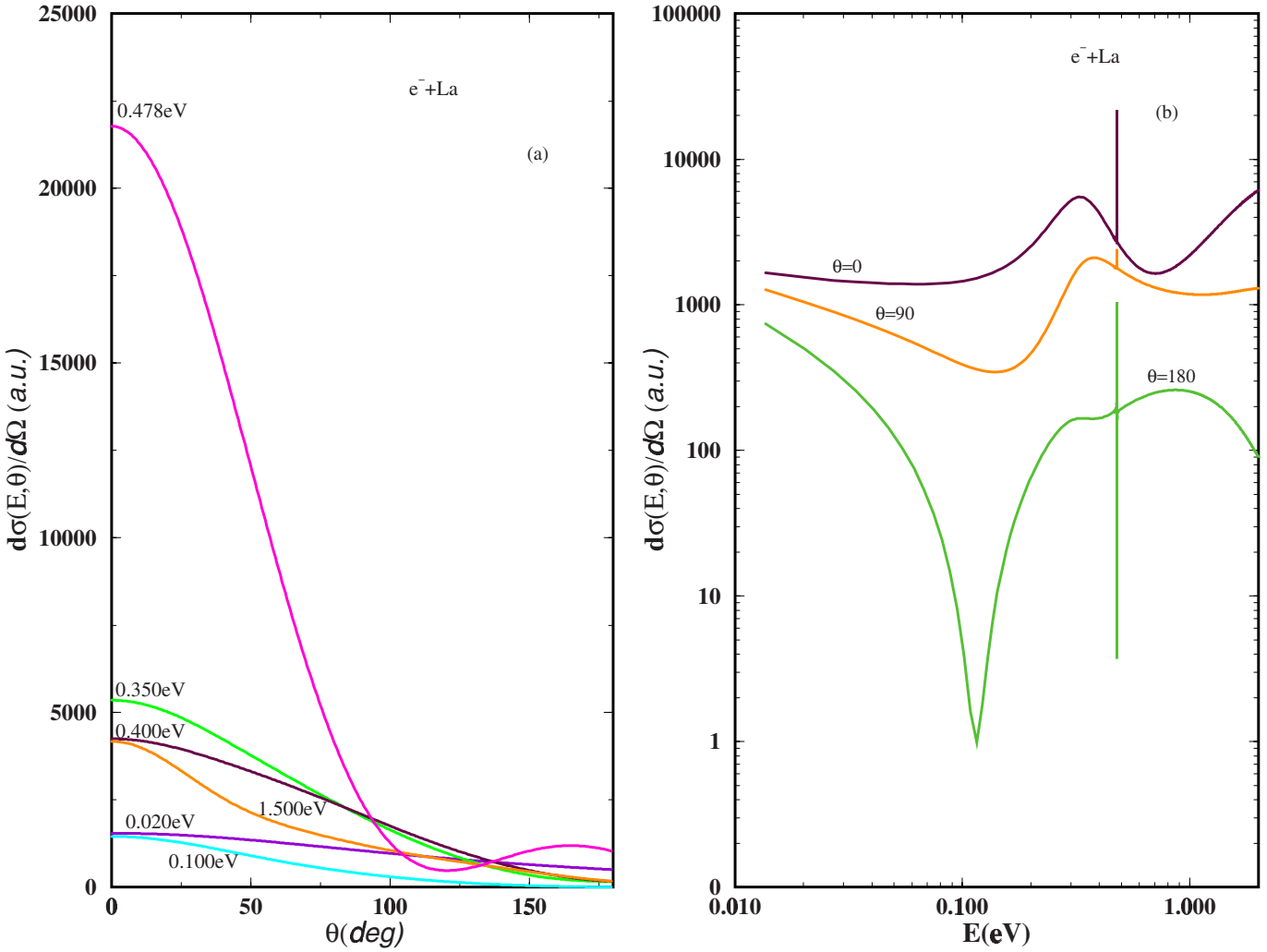

FIG. 3. (Color online) (a) Differential cross sections (a.u.) in scattering angle for electron elastic scattering by La atom at impact energies of 0.020, 0.100, 0.350, 0.4, 0.478, and 1.500 eV, showing the strong forward peaking at the binding energy of the resultant negative La^- ion. (b) Differential cross sections (a.u.) in impact energy for electron elastic scattering by La atom at scattering angles $\theta=0°$, 90°, and 180°. The position of the sharp resonances corresponds to the binding energy of the resultant negative La^- ion; the DCS critical minimum is also shown.

e^--Pt, e^--Sn, e^--Ge, etc. scatterings. This fixes the optimal value of b for the TF-type potential; the optimal values used for b in this paper are presented in Table I of Ref. [1] together with the EAs for the lanthanides, while the value of "a" was kept fixed at 0.2 for all the atoms.

The Schrödinger equation was solved for the electron in the field of the atomic target and numerically integrated for integer values of ℓ to a sufficiently large value of r. The S matrix was then determined and the differential cross section evaluated as the traditional sum over partial waves, with the index of summation being the integer angular momentum. This contrasts with the results of the Mulholland partial cross sections [1] which were obtained by integrating the Schrödinger equation for complex-angular-momentum values and real energy, thereby permitting the interpretation of the resonances as Regge resonances, including the differentiation between shape resonances and bound states through the close scrutiny of Im L. The following equation,

$$\Psi'' + 2\left(E - \frac{\ell(\ell+1)}{2r^2} - U(r)\right)\Psi = 0, \tag{6}$$

is solved with the boundary conditions:

$$\Psi(0) = 0,$$

$$\Psi(r) \sim e^{+i\sqrt{2E}r}, \quad r \to \infty. \tag{7}$$

Note that Eq. (7) defines a bound state when $k \equiv \sqrt{(2E)}$ is purely imaginary positive.

III. RESULTS

To facilitate the presentation and discussions of the electron elastic collisional DCSs for the lanthanides, also pointing out the subtle differences among them, we have divided the results into three general groups: (a) those that form com-

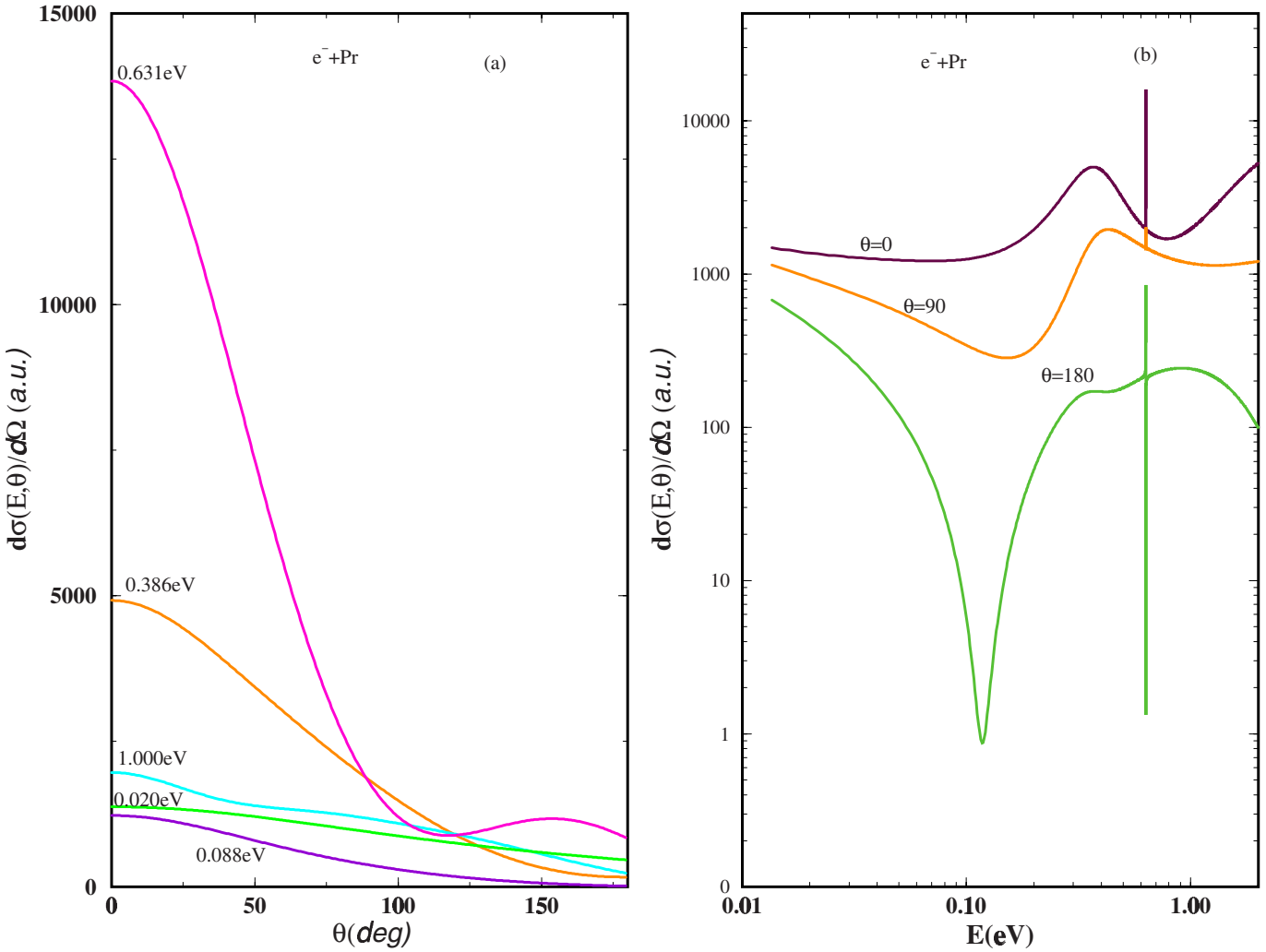

FIG. 4. (Color online) (a) Differential cross sections (a.u.) in scattering angle for electron elastic scattering by Pr atom at impact energies of 0.020, 0.088, 0.386, 0.631, and 1.000 eV, showing the strong forward peaking at the binding energy of the resultant negative Pr^- ion. (b) Differential cross sections (a.u.) in impact energy for electron elastic scattering by Pr atom at scattering angles $\theta=0°$, 90°, and 180°. The position of the sharp resonances corresponds to the binding energy of the resultant negative Pr^- ion; the DCS critical minimum is also shown.

plex open *d*- and *f*-subshell negative ions, such as Ce^- and Gd^- during the collisions, (b) those forming weakly bound negative ions with BEs <1.0 eV, such as La^-, Pr^-, Nd^-, Eu^-, and Dy^-, and (c) those that yield tenuously bound (BEs <0.1 eV) negative ions such as Tm^-. In the presentation of the results we will refer constantly to the paper [1] where the Regge trajectories, the EAs, and the relevant Re L and Im L are tabulated for these atoms.

A. Electron differential cross sections for Ce and Gd atoms

Figure 1(a) presents the DCSs in scattering angle for e^--Ce scattering at various impact energies varying from 0.02 to 1.5 eV. Most significant among these curves is that the largest value of the DCSs at $\theta=0°$ corresponds to the value of the resonance at 0.61 eV, the BE of the stable negative Ce^- ion [1]. Furthermore, the subsequent high value of the DCS corresponds to the value of the shape resonance at 0.373 eV. The DCS at 0.61 eV is highly peaked in the forward direction; the values of all the other DCSs below or above this value are much smaller. To clarify further the behavior of the DCSs with respect to their values and positions in E, we examine Fig. 1(b) where the DCSs in impact energy are plotted at $\theta=0°$, 90°, and 180° scattering angles.

At $\theta=0°$ scattering the shape resonance at 0.373 eV and the bound-state energy of the Ce^- (0.61 eV) are clearly well defined while at $\theta=90°$ the two peaks are significantly diminished in magnitude, with that at 0.373 eV being barely visible and a distinct minimum begins to develop. At $\theta=180°$ a deep minimum has developed in the DCS at about $E=0.10$ eV, defining the critical DCS minimum in the energy range $0\leq E\leq 1.0$ eV. The bound state energy peak is still clearly visible and is stronger but the peak corresponding to the shape resonance has completely disappeared. So an experimental investigation needs only to fix the detector at $\theta=0°$ or 180° to determine the EA of Ce unambiguously. However, for the shape resonance determination the most appropriate curve is the $\theta=0°$ one while for the DCS critical minimum the $\theta=180°$ curve is ideal for the experimental determination.

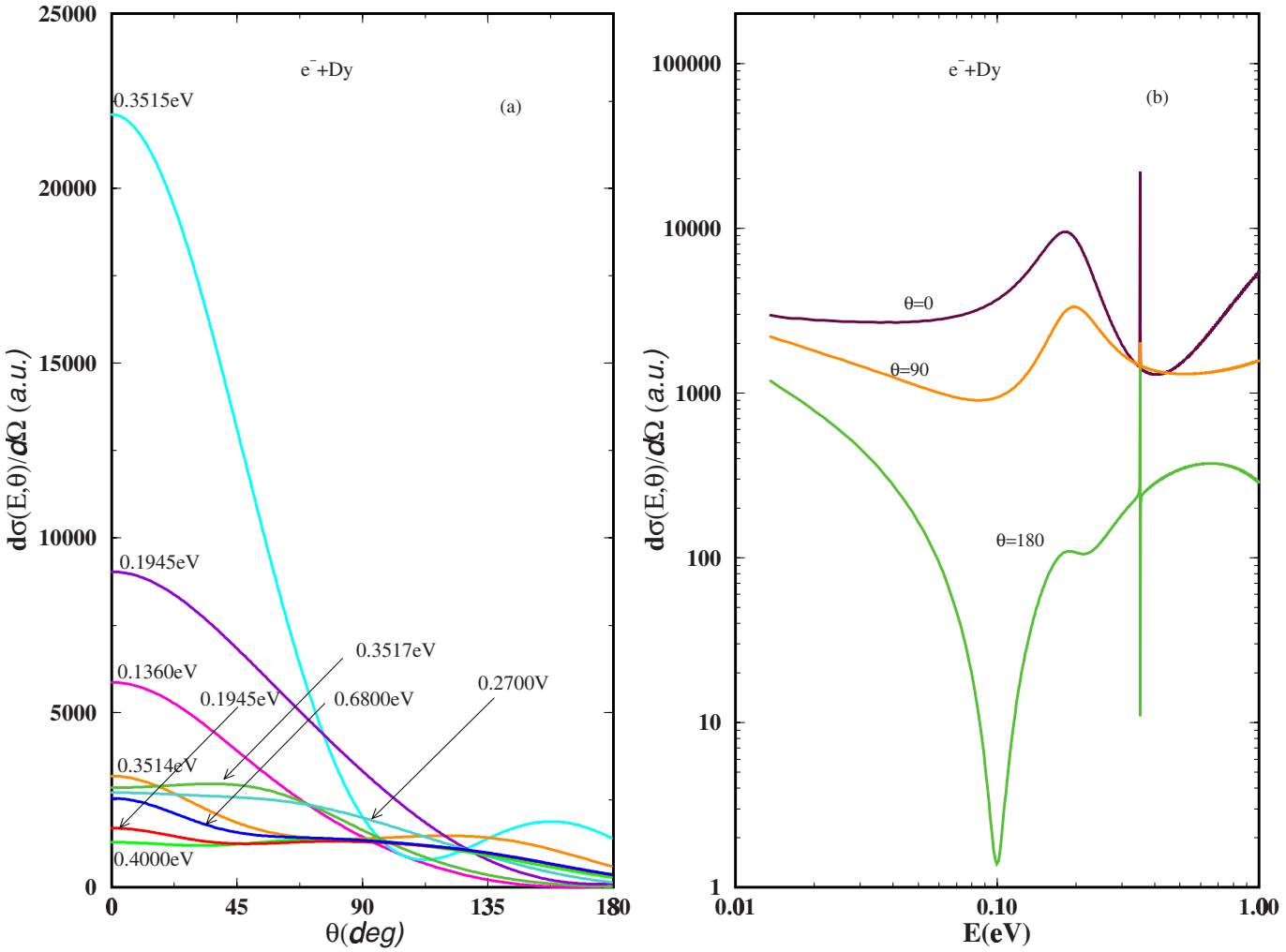

FIG. 5. (Color online) (a) Differential cross sections (a.u.) in scattering angle for electron elastic scattering by Dy atom at impact energies of 0.136, 0.3515, 0.3514, 0.3517, 0.1945, 0.270, 0.400, 0.540, and 0.680 eV, showing the strong forward peaking at the binding energy of the resultant negative Dy^- ion. (b) Differential cross sections (a.u.) in impact energy for electron elastic scattering by Dy atom at scattering angles $\theta=0°$, 90°, and 180°. The position of the sharp resonances corresponds to the binding energy of the resultant negative Dy^- ion; the DCS critical minimum is also shown.

Figure 2(a) shows the DCSs in scattering angles at various impact energies for the e^--Gd scattering. The results are similar to those for the e^--Ce scattering shown in Fig. 1(a). Here the largest value of the DCS occurs at $E=0.162$ eV in forward scattering. This value corresponds to the BE of the Gd^- ion formed during the collision. As in the case of the e^--Ce scattering the next maximum value of the DCS corresponds to the shape resonance at 0.027 eV. These values are clearly depicted in Fig. 2(b) where the DCSs in energy are plotted at $\theta=0°$, 90°, and 180°. The positions of the shape resonance and the bound state are quite pronounced in the figure. In contrast to the case of the e^--Ce scattering, shown in Fig. 1(b), for the e^--Gd scattering the shape resonance is visible at all the scattering angles of interest here, and the bound-state energy is dominant at $\theta=0°$, 90°, and 180°. Also, the position of the DCS critical minimum is at an energy value greater than 1.0 eV while the bound-state energy is closer to 0.1 eV. We note that the bound state manifests itself as an antiresonance at $\theta=180°$ and is well pronounced in the e^--Gd scattering. Clearly, although the two atoms have both open d and f subshells, the strong potential in Gd ($Z=64$) pulls the whole structure closer to threshold, in comparison to that of the e^--Ce scattering (Z of Ce is 58). Importantly, in e^--Gd scattering the structure of the DCS at $\theta=180°$ requires further careful investigation beyond 1.0 eV and below 0.01 eV for the delineation of its complete structure. Furthermore, the behavior of the DCSs versus θ for e^--Ce and e^--Gd scatterings are significantly different from each other; knowledge of one does not necessarily transfer to the other.

B. Electron differential cross sections for La, Pr, Dy, Nd, and Eu atoms

Figures 3–5 present the DCSs for the e^--La, e^--Pr, and e^--Dy scatterings, respectively. The results of Figs. 3(a), 4(a), and 5(a) resemble those of Fig. 1(a) with the largest values of the DCSs found in forward scattering at electron-impact energies of 0.478, 0.631, and 0.3515 eV, respectively, and corresponding to the BEs of the negative ions La^-, Pr^-,

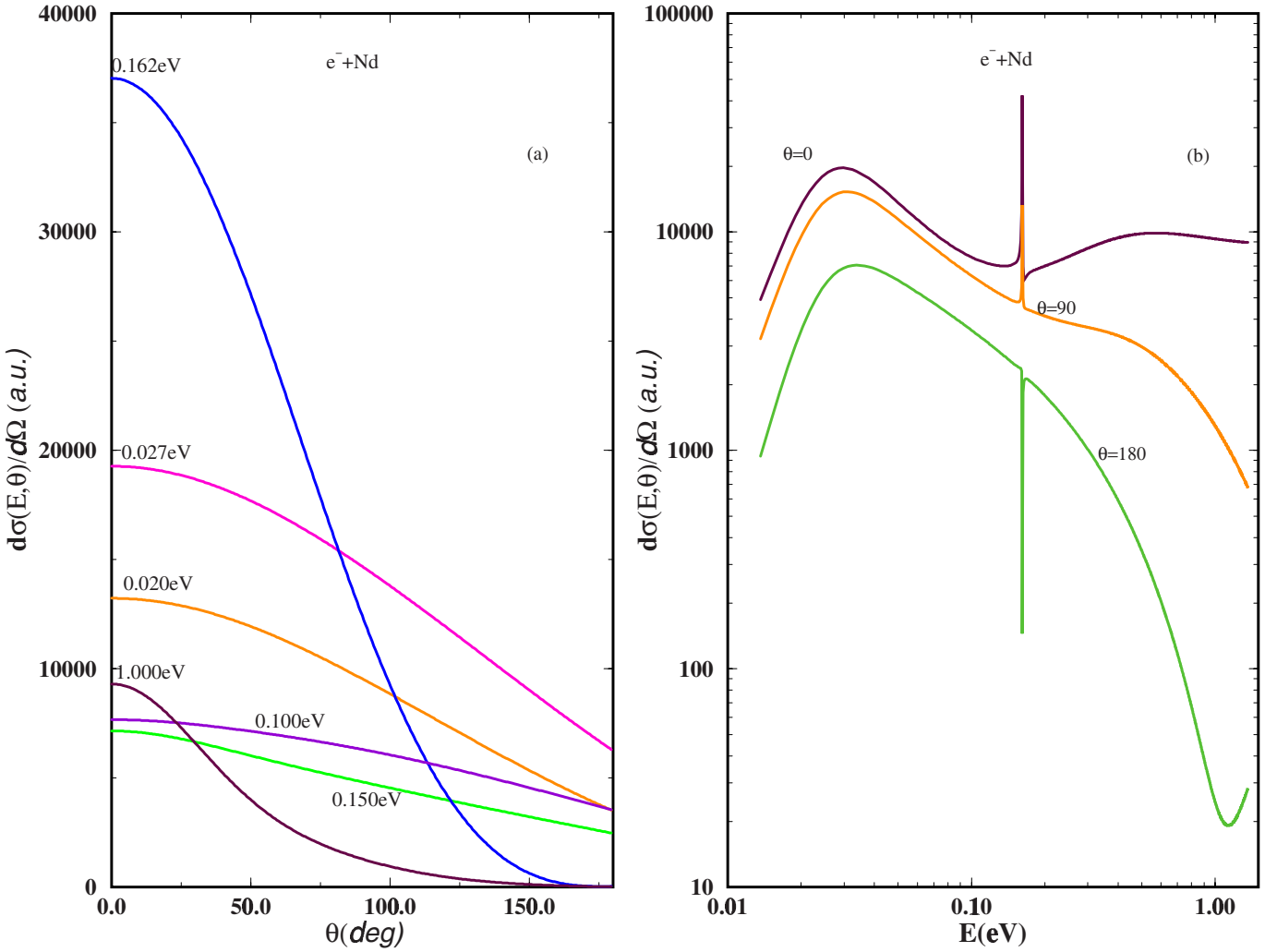

FIG. 6. (Color online) (a) Differential cross sections (a.u.) in scattering angle for electron elastic scattering by Nd atom at impact energies of 0.020, 0.027, 0.100, 0.150, 0.162, and 1.000 eV, showing the strong forward peaking at the binding energy of the resultant negative Nd^- ion. (b) Differential cross sections (a.u.) in impact energy for electron elastic scattering by Nd atom at scattering angles $\theta=0°$, 90°, and 180°. The position of the sharp resonances corresponds to the binding energy of the resultant negative Nd^- ion; the DCS critical minimum is also shown.

and Dy^- formed during the collisions. Note the extreme sensitivity of the BE of the Dy^- negative ion in comparison to those of the former two. As E increases or decreases with respect to the BEs, the next values of 0.35, 0.386, and 0.194 eV correspond to the shape resonances of the La, Pr, and Dy atoms [1], respectively. These were carefully analyzed and discussed in [1]. Below and above these values the DCSs are drastically lower just as in the e^--Ce and e^--Gd scatterings. Figures 3(b), 4(b), and 5(b) show the corresponding DCSs in impact energy at $\theta=0°$, 90°, and 180°. These also resemble those of the e^--Ce and e^--Gd scatterings, including the positions of the DCS critical minima at about 0.1 eV. In all the e^--La, e^--Pr, and e^--Dy scatterings the resonances and antiresonances at $\theta=90°$ are quite strong. However, the DCS critical minima and the bound-state resonances should be readily differentiated through the observation of their widths; the latter have very narrow widths while the former have significantly wider widths by comparison.

It is noted that the scattering DCSs at 180° for these atoms could be useful for the experimental determination of both the BEs and the DCS critical minima. However, the measurement of the energy positions of the shape resonances and the BEs in the e^--La, e^--Pr, and e^--Dy scatterings can best be achieved at $\theta=0°$ or near it. Because the variation in the DCSs is not so rapid in the energy region near $\theta=0°$, the shape resonances and the BEs could be measured without much errors. This analysis is consistent with that obtained from the TCSs [1]. The energy positions of the resultant shape resonances are quite close to one another for these systems. Although the atoms La, Pr, and Dy have significantly different electron configurations, viz. La[Xe]$5d^16s^2$, Pr[Xe]$4f^36s^2$, and Dy[Xe]$4f^{10}6s^2$, their electron attachment is determined by Re $L=4$ and their shape resonances by Re $L=2$ (see Ref. [1]). This only serves to emphasize that for electron elastic scattering by the lanthanide atoms each case must be calculated separately because of the generally complex and subtle interactions among the many diverse electron configurations involved in the lanthanide atoms. For the e^--La, e^--Pr, and e^--Dy scatterings the DCS scattering curves corresponding to the shape resonances, see Figs. 3(a),

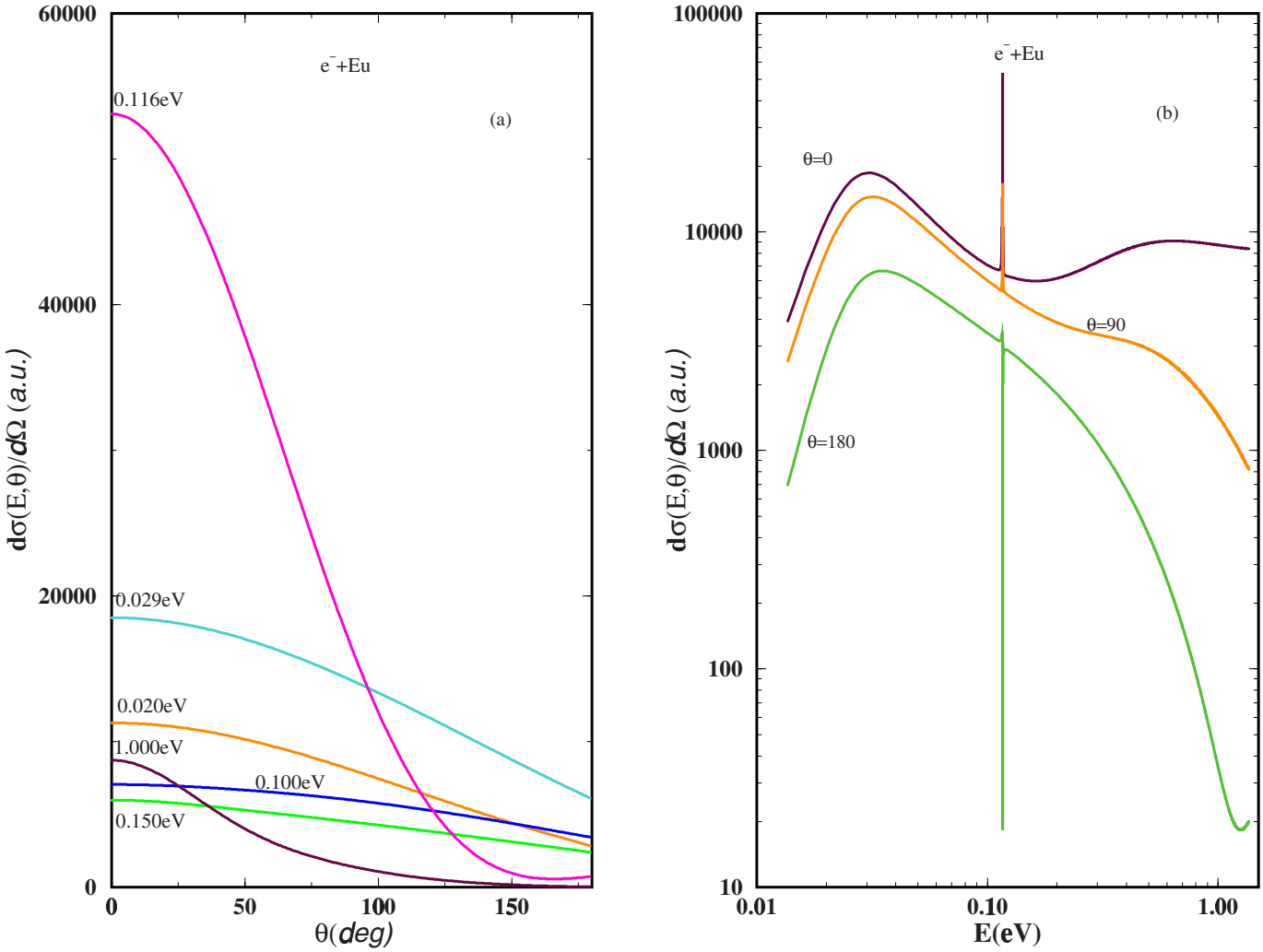

FIG. 7. (Color online) (a) Differential cross sections (a.u.) in scattering angle for electron elastic scattering by Eu atom at impact energies of 0.020, 0.029, 0.100, 0.116, 0.150, and 1.000 eV, showing the strong forward peaking at the binding energy of the resultant negative Eu^- ion. (b) Differential cross sections (a.u.) in impact energy for electron elastic scattering by Eu atom at scattering angles $\theta=0°$, 90°, and 180°. The position of the sharp resonances corresponds to the binding energy of the resultant negative Eu^- ion; the DCS critical minimum is also shown.

4(a), and 5(a), are virtually flat over the approximate angular range $0 \leq \theta \leq 10°$ so that measurement of the shape resonance energies could be accomplished without introducing much errors. Interestingly, the DCS curves in angle corresponding to the BEs of the resultant negative ions La^-, Pr^-, and Dy^- exhibit the only structure with minima at about 118°, 116°, and 110°, respectively. In all these cases, second maxima in addition to those at $\theta=0°$ also appear around 160°. These present interesting challenges for experimentalists.

Although the electronic structures of Nd[Xe]$4f^4 6s^2$, Eu[Xe]$4f^7 6s^2$, and Gd[Xe]$4f^7 5d 6s^2$ are significantly different from one another, the structure of the e^--Nd, e^--Eu, and e^--Gd scattering DCSs are remarkably similar to one another, Figs. 6, 7, and 2, respectively. In particular, the maxima of the DCSs in scattering angle at $\theta=0°$ correspond to the BEs of the negative ions Nd^-, Eu^-, and Gd^- formed during the collisions as resonances. These are, respectively, 0.162, 0.116, and 0.137 eV, see also [1]. Above and below these values the DCSs drop down in magnitude considerably to the energy values of the shape resonances at 0.027, 0.029, and 0.034 eV, respectively. At other energies the DCSs at $\theta=0°$ are significantly lower so that it is simpler to identify either the bound-state energies or the shape resonance energies as seen from Figs. 6(a), 7(a), and 2(a). Here too measuring around $\theta=0°$ within the range $0 \leq \theta \leq 10°$ could yield reasonably good values of the BEs for the Nd^-, Eu^-, and Gd^- negative ions as well as the shape resonances.

Figures 6(b), 7(b), and 2(b) present the DCSs in energy for the e^--Nd, e^--Eu, and e^--Gd scatterings, respectively, at $\theta=0°$, 90°, and 180°. As before the dramatically sharp resonances at energies of 0.162, 0.116, and 0.137 eV at all these scattering angles are manifestations of the bound-state energies of the negative ions Nd^-, Eu^-, and Gd^- formed during the collisions as resonances. These are preceded by the broad peaks centered on 0.027, 0.029, and 0.034 eV at all the angles, corresponding to the positions of the shape resonances. The former set of values correspond to electron at-

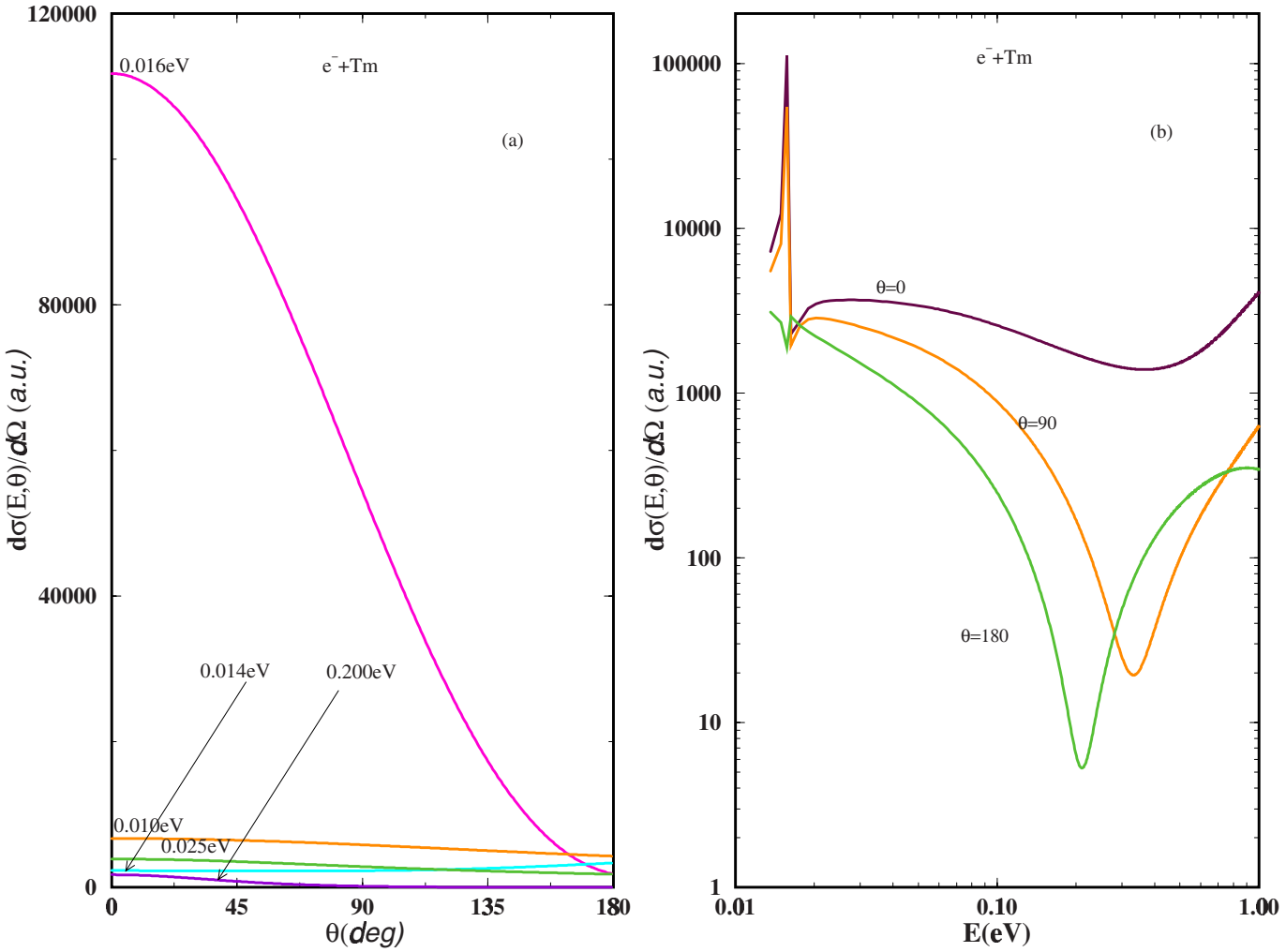

FIG. 8. (Color online) (a): Differential cross sections (a.u.) in scattering angle for electron elastic scattering by Tm atom at impact energies of 0.010, 0.014, 0.016, 0.025, and 0.200 eV, showing the strong forward peaking at the binding energy of the resultant negative Tm^- ion. (b) Differential cross sections (a.u.) in impact energy for electron elastic scattering by Tm atom at scattering angles $\theta=0°$, 90°, and 180°. The position of the sharp resonances corresponds to the binding energy of the resultant negative Tm^- ion; the DCS critical minimum is also shown.

tachment of Re $L=3$ [1] in forming the bound states of the negative ions while the shape resonances are characterized by Re $L=1$ electron attachment [1]. Here the BEs of the resultant negative ions could readily be experimentally determined at all the scattering angles depicted in Figs. 6(b), 7(b), and 2(b). For the e^--Nd scattering the DCS critical minimum appears at about 1.0 eV in the $\theta=180°$ curve, while for the e^--Eu and e^--Gd scatterings the DCSs critical minima are at values of E beyond the 1.0 eV energy range of interest in this paper.

It should be noted however that the positions of the bound-state energies of the resultant negative ions are sensitive to the electronic configurations of their atoms. When we compare the BEs of the negative ions Nd^- and Eu^- formed during the collisions, we see the importance of the f orbital in the BE of the Eu^- ion; it leads to a lower BE value of the resultant negative ion in comparison with that of the Nd^- ion, whose atom has a $4f^4$ rather than the $4f^7$ in the atom of Eu^-. The influence of the $5d$ orbital on the BE of the Gd^- negative ion formed during the collision is best seen by comparing the results of Figs. 2(b) and 7(b). The presence of the $5d$ orbital slightly increases the BE of the Gd^- ion compared with that of the Eu^- negative ion whose atom has no $5d$ orbital. However, this $5d$ orbital does not appear to have any significant influence on the position of the DCS critical minimum.

C. Electron differential cross sections for Tm atom

The Tm atom is the last of the lanthanide atoms, with a completely filled f subshell. The BE of its negative ion, formed during the collision, has been determined to be the lowest of the lanthanides [1]. Figure 8(a) depicts this situation very well, with the maximum in the DCS at $\theta=0°$ corresponding to the BE of the Tm^- ion of 0.016 eV. The values of the DCSs above and below this value are orders-of-magnitude smaller. For the case of e^--Tm scattering, it would be simpler to experimentally measure the BE of the Tm^- negative ion through the measurement of the DCS at $\theta=0°$. Granted, it is very difficult to directly measure the DCSs at $\theta=0°$. However, over a range of scattering angles, roughly

between 0° and 10° the BE of the Tm^- negative ion does not vary significantly, thus providing an opportunity to measure the BE of the Tm^- ion without introducing much errors.

In Fig. 8(b) is demonstrated the variation in the DCS with electron-impact energy for Tm at $\theta=0°$, 90°, and 180°. Just as in the case of the e^--Gd scattering, measuring at $\theta=0°$ or 90° yields unambiguously the BE of the Tm^- negative ion although with utmost care the BE could also be determined at $\theta=180°$ if this is the only experimentally accessible scattering angle. The DCS critical minimum appears at above 0.22 eV on the $\theta=180°$ scattering curve. Note the resemblance of the resonance structure in Fig. 8(b) to that of Fig. 2(b). Because of the high Z value of Tm compared to that of Gd, the whole resonance structure of Fig. 2(b) has been pulled closer toward threshold, revealing the DCS critical minimum in the e^--Tm scattering at 180°; this minimum is above the 1.0 eV value in the e^--Gd scattering. We note that the DCS depicted in Fig. 8(b) clearly resembles those for the e^--Hf and e^--Lu scatterings depicted in Figs. 1 and 2 of [4]. At $\theta=0°$ and 90° the resonance corresponding to the bound state of the negative Tm^- ion is dominant. However, at $\theta=180°$ the resonance is barely visible but at this scattering angle the DCS critical minimum appears at about 0.22 eV. Note that the minima in the e^--Hf and e^--Lu scatterings are also expected to appear around this energy value. The results of [4] were terminated at $E=0.1$ eV just before the DCS critical minima were reached in the e^--Hf and e^--Lu scatterings. To measure the BE of the Tm^- ion the experimenter needs only to measure at $\theta=90°$ the DCS as a function of E. This would also lead close to the position of the DCS critical minimum. A switch to measurement on the $\theta=180°$ curve and decreasing the impact energy would then yield the value of the DCS critical minimum.

IV. SUMMARY AND CONCLUSIONS

We have used a Thomas-Fermi-type potential incorporating the crucial core-polarization interaction in the Schrödinger equation to calculate the scattering amplitude and hence the DCSs to explore the near-threshold electron attachment to the representative lanthanide atoms La, Ce, Pr, Nd, Eu, Gd, Dy, and Tm through the investigation of the elastic DCSs in scattering angle in the electron energy range $0 \leq E \leq 1$ eV, keeping below any thresholds to avoid their influence. Generally, the electron DCSs for these atoms are found to be characterized by dramatically sharp resonances in forward scattering, whose energy positions are identified with the BEs of the negative ions formed during the collisions as Regge resonances. In particular, the resonances are enhanced at $\theta=0°$ and 90° (DCSs manifesting as very sharp peaks) when the electron-impact energy corresponds to the BEs of the resultant negative ions formed during the collisions. This gives a more direct, simple, and unambiguous as well as reliable alternative method to the traditional one of using the Wigner threshold law for the experimental determination of BEs of ground-state negative ions. We also demonstrated that shape resonances and the DCSs critical minima can be determined from the electron elastic DCSs for these lanthanide atoms.

We conclude by noting that although both Ce and Gd atoms have open d and f subshells, the shapes of their electron elastic DCSs, particularly those in E, are completely different from each other. This implies that each system requires careful individual investigation. It is hoped that this presentation and discussions of the electron-lanthanide atom elastic-scattering DCSs in both scattering angle and electron-impact energy will provide the impetus toward a concerted effort to experimentally determine reliable EA values of atoms in general and the lanthanides in particular.

ACKNOWLEDGMENTS

Research was supported by U.S. DOE, Division of Chemical Sciences, Office of Basic Energy Sciences, Office of Energy Research and the CAU CFNM, NSF-CREST Program. D.S. is supported through a EPSRC-GB (U.K.) Grant. The computing facilities at the Queen's University of Belfast, U.K. and of DOE Office of Science, NERSC are greatly appreciated.

[1] Z. Felfli, A. Z. Msezane, and D. Sokolovski, Phys. Rev. A **79**, 012714 (2009).
[2] D. Sokolovski, Z. Felfli, S. Yu. Ovchinnikov, J. H. Macek, and A. Z. Msezane, Phys. Rev. A **76**, 012705 (2007).
[3] P. D. Burrow, J. A. Michejda, and J. Comer, J. Phys. B **9**, 3225 (1976).
[4] Z. Felfli, A. Z. Msezane, and D. Sokolovski, Phys. Rev. A **78**, 030703(R) (2008).
[5] A. R. Milosavljevic, D. Sevic, and B. P. Marinkovic, J. Phys. B **37**, 4861 (2004).
[6] J. E. Sienkiewicz, S. Telega, P. Syty, and S. Fritzsche, Phys. Lett. A **293**, 183 (2002).
[7] B. Predojevic, D. Sevic, V. Pejcev, B. P. Marinkovic, and D. M. Filipovic, J. Phys. B **38**, 1329 (2005).
[8] V. I. Kelemen, M. M. Dovhanych, and E. Yu. Remeta, J. Phys. B **41**, 035204 (2008).
[9] V. I. Kelemen, E. Yu. Remeta, and E. P. Sabad, J. Phys. B **28**, 1527 (1995).
[10] Z. Felfli, A. Z. Msezane, and D. Sokolovski (unpublished).
[11] E. Yu. Remeta, V. I. Kelemen, Yu. Yu. Bilak, and L. L. Shimon, Ukr. J. Phys. **47**, 423 (2002).
[12] S. M. O'Malley and D. R. Beck, Phys. Rev. A **74**, 042509 (2006).
[13] Z. Felfli, A. Z. Msezane, and D. Sokolovski, J. Phys. B **41**, 041001 (2008).
[14] C. W. Walter, N. D. Gibson, C. M. Janczak, K. A. Starr, A. P. Snedden, R. L. Field III, and P. Andersson, Phys. Rev. A **76**, 052702 (2007).
[15] A. M. Covington, D. Calabrese, J. S. Thompson, and T. J. Kvale, J. Phys. B **31**, L855 (1998).
[16] S. M. O'Malley and D. R. Beck, Phys. Rev. A **77**, 012505 (2008).
[17] S. M. O'Malley and D. R. Beck, Phys. Rev. A **78**, 012510 (2008).
[18] S. Belov, N. B. Avdonina, Z. Felfli, M. Marletta, A. Z. Msezane, and S. N. Naboko, J. Phys. A **37**, 6943 (2004).